

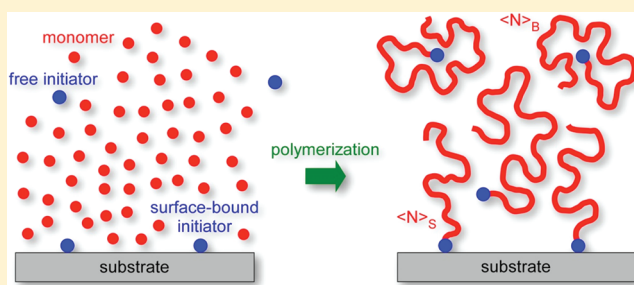
Computer Simulation of Concurrent Bulk- and Surface-Initiated Living Polymerization

Salomon Turgman-Cohen[†] and Jan Genzer*

Department of Chemical & Biomolecular Engineering, North Carolina State University, Raleigh, North Carolina 27695-7905, United States

S Supporting Information

ABSTRACT: We use Monte Carlo simulation implementing the bond fluctuation model formalism in the canonical (NVT) ensemble to study living polymerization initiated concurrently in bulk and on flat substrates. Our results reveal that the molecular weights and molecular weight distributions of both classes of polymers depend on the grafting density of the surface-bound polymers (σ) and the fraction of polymers on the surface (η) relative to that in bulk. In general, polymer grafts on the surface possess lower molecular weight and higher polydispersity index compared to their bulk counterparts. The difference between the molecular weight of the two populations of polymers decreases with decreasing σ and increasing η . Our work provides evidence that the common practice of using the molecular weight of bulk-initiated polymers in estimating the grafting density of polymeric anchors on flat substrates is not generally valid.



INTRODUCTION

Decorating material surfaces with polymeric grafts has become a routine method for generating functional materials for various applications, including, friction, biocompatibility, self-assembly, responsive materials, and many others.^{1–7} The parameters that govern the performance of macromolecular tethers are the polymer chemical composition, topology (i.e., linear or branched), grafting density, and molecular weight. The past decade witnessed enormous progress in generating and probing the physicochemical characteristics of such surface-anchored polymer assemblies. Two general classes of methods have been developed for the preparation of polymeric tethers on material surfaces.^{8–10} In the “grafting onto” technique, polymers are synthesized in bulk and grafted (chemically or physically) to the substrate of interest. This method benefits from knowing a priori the characteristics of the polymers, i.e., chemical composition, molecular weight (M_n), and molecular weight distribution (MWD), before they get grafted to the substrate. However, entropic constraints during chain grafting limit the grafting density (σ) of polymeric tethers to moderate values. This limitation of the “grafting onto” method can be technically eliminated by synthesizing grafted polymers directly from surfaces by the so-called “grafting from” methodology. Here, the surfaces are decorated with polymerization initiators and polymers grow from these active centers upon exposure to a solution of monomer, catalyst, and/or solvent. While the “grafting from” technique can in principle yield grafted systems with higher σ than the “grafting onto” process, it is not without flaws. Specifically, the structure of the brush near the surface, its

molecular weight, and MWD are not known a priori and have to be established after brush formation.

A typical method for determining the molecular weight of surface-grown polymers ($M_{n,s}$) and their MWD involves cleaving the chains from the substrate by some chemical treatment, collecting them, and testing them with size exclusion chromatography (SEC).^{11–13} While for grafted polymers grown from convex (i.e., particle) or concave (i.e., pore) substrates with high surface areas this methodology is feasible, it is generally not applicable for grafts polymerized from flat substrates because the amount of material cleaved from the surface is not sufficient for SEC analysis. Hence, most papers describing the growth of polymeric grafts from flat substrates report the properties of brushes in terms of their dry thickness (h). These data alone, however, do not provide direct means of determining the $M_{n,s}$ of the grown polymer (nor does it say anything about the MWD) unless information about σ is available. Unfortunately, this is not the case in most situation because determining σ is even more challenging than measuring M_n . To solve this dilemma, one typically conducts simultaneous polymerization initiated both on the surface and in the bulk and assumes that both bulk- and surface-initiated polymers grow at

Received: December 10, 2011

Revised: January 29, 2012

Published: February 8, 2012

similar rates. By assuming that $M_{n,S} \approx M_{n,B}$, one can calculate σ from

$$\sigma = \frac{h\rho N_a}{M_{n,S}} \quad (1)$$

In eq 1, which can be derived simply by conservation of mass arguments, ρ is the density of the polymer and N_a is Avogadro's number. The objective of this work is to determine the validity of the $M_{n,S} \approx M_{n,B}$ assumption and to compare the MWDs of the two classes of macromolecules.

The synthesis of surface-grafted polymers is often accomplished by controlled radical polymerization (CRP) methods.^{1,11,14,15} Within this class of reactions, atom transfer radical polymerization (ATRP) is a widely employed reaction scheme^{1,16} due to its compatibility with an extensive library of monomers, the living character of the reaction (allowing the creation of block copolymers), insensitivity to impurities (compared to free radical or ionic polymerization techniques), the ability to control the average molecular weight, and to obtain polymers with low PDI in bulk. In the context of ATRP, the presence of free initiators in solution can have an effect on the intrinsic growth kinetics of the surface polymers. Surface reactions, especially those from planar substrates, produce very small amounts of the deactivating species (i.e., CuX_2 in ATRP where $\text{X} = \text{Cl}$ or Br) leading to loss of control due to excessive terminations at the early stages of the polymerization. Sacrificial (free) initiators added to the bulk solution increase the concentration of the deactivating species, thus restoring control to the reaction.^{1,17–19} A second way in which free initiators may affect polymerization from surface-bound initiators involves competing with the surface-bound polymers for the available monomers. It is possible for surface- and bulk-grown polymers to exhibit different polymerization rates leading to dissimilar molecular weights and PDIs for these two populations of polymers. Such a difference invalidates the application of eq 1 for the characterization of the grafted polymer layers because the assumption that $M_{n,S} \approx M_{n,B}$ becomes unfounded.

This study focuses on investigating the competition between polymerization initiated in bulk and concurrently on flat impenetrable surfaces. Initial findings pertaining to this goal have been presented recently.²⁰ Here we elaborate on the system parameters that affect the characteristics of polymers grown simultaneously from surfaces and in bulk. Specifically, we plan to address how the molecular weight and the MWD of both classes of macromolecules (i.e., bulk- and surface-initiated) depend on the initiator grafting density (σ), fraction of polymers on the surface (η) relative to the total number of polymers grown, and the initial number of free monomers in the simulation box (M_0). We neglect any effects that the presence of bulk initiators may have on the activation/deactivation and on the buildup of deactivating species since we incorporate these processes in our simulations implicitly. This is to say that the polymerizations studied herein remain living (i.e., without termination or chain transfer) and controlled, and the value of η has no effect on the intrinsic kinetics of the polymerization process. In addition, we assume that bulk and surface polymers possess equal probabilities of undergoing activation and deactivation reactions and of reacting with nearby monomers.

SIMULATION MODEL AND ALGORITHM

We employ the Monte Carlo (MC) algorithm in the canonical (NVT) ensemble described in our earlier work^{20–22} and the bond fluctuation model (BFM)^{23,24} under good solvent conditions to investigate the effects of M_0 , η , and σ on the simultaneous polymerization of bulk- and surface-initiated polymers. Briefly, in every MC step either a reaction or a motion depends on a preselected reaction probability, P_r (chosen 0.01 for this study). If motion is selected, a typical BFM single monomer move is attempted. In the case of reaction, a reaction is attempted between a randomly selected polymer and one of its nearest-neighbor free monomers. The randomly selected polymer may only react if it is active at a given time. Similar to the ATRP mechanism, in which only a certain fraction of polymers is “living” for a certain period of time, we specify the lifetime of active polymers (LT) and fraction of living polymers (FLP) that can undergo reaction (i.e., initiation or propagation in our case). In the current simulations every polymer has equal probability of initiating or reacting regardless of it being a bulk- or a surface-initiated polymer. Additional details of the simulation can be found in our previous publications.^{20–22}

The initial number of total initiators (combined bulk and surface) remains constant ($I_0 = 400$). By choosing η , we therefore vary the number of bulk and surface polymers (i.e., for $\eta = 0$ only bulk polymerization takes place while $\eta = 1$ polymerization occurs only on the substrate). In order to vary σ and η independently, we alter the dimensions of the lattice in the lateral ($L_x = L_y$) and vertical (L_z) dimensions independently while keeping the total volume of the lattice at $\approx 5 \times 10^5$ cubic lattice units. In order to vary σ , we employ the procedure for resizing the lattice described in our previous publications.^{20,22} Additional variations in the lattice sizes are needed when keeping σ constant while varying η . We resize the lateral dimensions of the lattice as the number of polymers on the surface varies to maintain a constant σ . We also vary M_0 in order to explore the effects of free monomer density on polymerization. Varying M_0 should reveal any possible effects associated with diffusion limitation during the course of the polymerization reaction. The surfaces of lattices corresponding to various σ and η investigated and the positions of the initiator sites (i.e., the X – Y plane at $L_z = 0$) are depicted in Figure S1 of the Supporting Information. Some of the lattices investigated possess large aspect ratios ($L_z/L_x = 62.7$ for $\eta = 6\%$ and $\sigma = 0.25$), which might confine the polymers and affect the polymerizations. To verify that the large lattice aspect ratio does not affect the properties of the growing polymers, we compared the PDIs of bulk polymers ($\eta = 0\%$) grown in lattices with low ($L_z/L_x = 1$) and high ($L_z/L_x = 62.7$) aspect ratios as a function of conversion and number-average molecular weight. Our results (not shown here) determined that the molecular weights and PDIs were equivalent for all lattice aspect ratios tested.

The living nature of polymerizations described by our algorithm is achieved by omitting reactions that lead to chain termination or chain transfer. Hence, we only consider the initiation and propagation steps. To test the effect that diffusion and the scarcity of monomers may have in our results, we perform simulations at varying values of M_0 , which requires adjustments to the parameters affecting the reaction kinetics (cf. Table 1). The parameters requiring adjustment are P_r and LT. If we increase the initial number of free monomers in the

Table 1. Parameters Adjusted in Order To Change M_0 Correctly

M_0	beads	P_r	LT
6 250	7 050	0.0187	535
12 500	13 300	0.0100	1000
25 000	25 800	0.0052	1930

simulation while keeping P_r constant, there will be, on average, a lower fraction of total beads attempting to move between attempted reaction steps. This is equivalent to a change in the relative rates of reaction and motion, an undesirable consequence of a simple increase in M_0 . We therefore adjust P_r depending on the value of M_0 in order to keep the relative rates of reactions and motions constant. For instance, if M_0 equals 12 500 and $P_r = 0.01$, there will be on average 99 attempted motions for every attempted reaction, which corresponds to 0.74% of the beads attempting a move. In contrast, for $P_r = 0.01$ and $M_0 = 25\,000$, 0.38% of the beads would undergo attempted motion. To take this effect into account, we use the $M_0 = 12\,500$ and $P_r = 0.01$ simulations as a benchmark, and for other values of M_0 , we adjust P_r to maintain the fraction of beads attempting a move between attempted reactions equal to 0.74% of the total beads (cf. Table 1). The value of LT also affects the kinetics of the polymerization reaction in our simulations. If P_r adjustments are needed to account for the varying number of beads, then LT corrections are necessary to account for the unintended consequences of varying P_r . As P_r is adjusted, the average number of reactions occurring within a living polymer cycle varies proportionally. For instance, if P_r equals 0.01 or 0.10 and LT = 1000, there will be on average 10 or 100 attempted reactions, respectively, every living cycle. Kinetic theories of CRP reactions have shown that the number of propagations per living cycle is an important parameter in the CRP scheme and that it can have significant effects on the molecular weight distribution of the resulting polymers.²⁵ Adjustments in P_r and LT are therefore needed to compare systems with different M_0 . In the MC simulations described here, we use the values of P_r and LT listed in Table 1.

The initial configurations comprise equidistant arrays of initiators on the flat surface (cf. Figure S1 in Supporting Information). The bulk initiators and free monomers are distributed regularly throughout the lattice. Each initiator corresponds to two BFM monomers, of which one can undergo initiation if approached by a free monomer. For surface bound initiators, the noninitiating site is grafted firmly to the surface and is not allowed to move during the simulation. We pre-equilibrate the configurations thus constructed for at least 1×10^5 attempted MC moves per bead (MCPB), yielding a random spatial distribution of free initiators and monomers on the lattice. The randomly distributed configurations serve as an input to the reactive simulations. As mentioned earlier, we model “living” polymerization conditions by disabling termination and chain transfer reactions. We obtain averages of the number-average molecular weight and the PDI by repeating each simulation five times and sampling the system at regular values of the free monomer conversion (X_m). Prior to the initialization of the reactive MC algorithm, we perform a final short equilibration consisting of 1×10^6 attempted MC moves. The reactive MC scheme described earlier¹⁶ then begins and continues until either 80% of the free monomer is exhausted (i.e., polymerized) or a predetermined maximum number (1×10^9) of MCS elapses. For some of the lattices in Table 1 the distance between the substrate and the opposing impenetrable wall (L_z) is very small. To prevent interaction of the tethered polymers with the opposite wall, it is necessary to truncate some of the data sets (Table SI, Supporting Information). Because the weight of the monomers is unity, we express the molecular weights of the bulk- and surface-grown polymers in terms of the average number of monomers in the respective polymers, i.e., $\langle N \rangle_B$ and $\langle N \rangle_S$.

RESULTS AND DISCUSSION

To elucidate the effects of η and σ , we monitor the average molecular weight as a function of X_m at $M_0 = 25\,000$ independently for bulk- and surface-based polymers and compare them to the $\eta = 0$ or 100% (cf. Figure 1). Note that pure bulk or surface polymers exhibit identical average molecular weights as a function of conversion, as expected

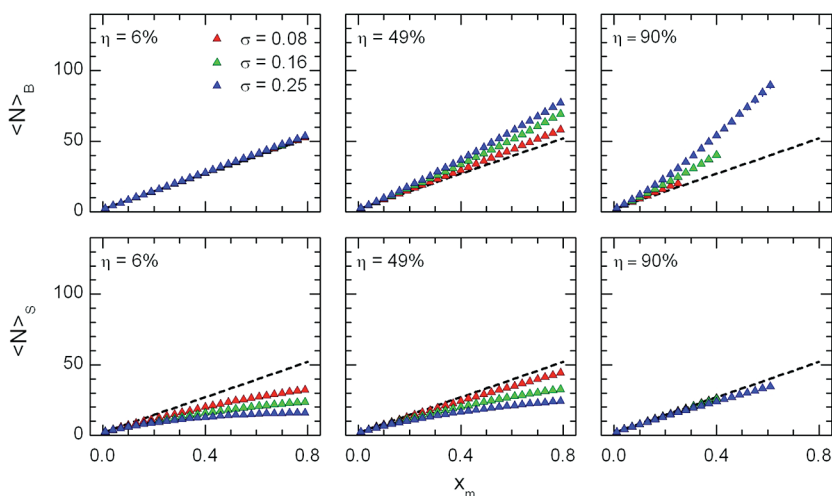


Figure 1. Average molecular weight for bulk (top row) and surface (bottom row) polymers as a function of monomer conversion with initial number of monomers (M_0) of 25 000; percentages of surface polymers (η): 6% (left column), 49% (middle column), and 90% (right column); grafting densities of initiators (σ): 0.08 (red), 0.16 (green), and 0.25 (blue). The black dashed lines represent the conditions corresponding to $\eta = 0\%$ (top) and 100% (bottom). The $\eta = 90\%$ data are truncated because the brush starts interacting with the opposite impenetrable surface.

(dashed lines). The average molecular weight of bulk-grown macromolecules increases linearly at $\eta = 6\%$, as one would expect from polymerizations in which only bulk polymers are grown ($\eta = 0\%$, black dashed lines). With η increasing from 6% to 90%, $\langle N \rangle_B$ deviates from the dashed line and becomes larger than expected. The deviation for $\sigma = 0.08$ is small, indicating that polymers growing sparsely from surfaces propagate at a similar pace to their bulk counterparts. The magnitude of the deviation depends on σ , however, indicating that the surface-bound initiators affect the properties of the bulk-grown polymers under these conditions. Namely, increasing the density of surface-bound initiators increases the molecular weight of the bulk-grown polymers. The surface-initiated polymers exhibit the opposite trend. Specifically, the data lie below the black line indicating that shorter polymers are produced relative to $\eta = 100\%$ case (i.e., polymerization is initiated only from the surface). While for the surface-grown polymers the deviation between the $\eta = 90\%$ and the dashed line is very small, the deviation becomes larger as η decreases from 90% to 6%, indicating that at low η the polymers initiating from the surface grow at a slower pace than the bulk-initiated macromolecules. Increasing σ tends to enlarge the deviation from the $\eta = 100\%$ line, suggesting that the larger the σ , the slower the rate of surface-initiated polymerization. Furthermore, at $\eta = 6\%$ and $\sigma = 0.25$, $\langle N \rangle_S$ reaches a plateau at approximately $X_m = 0.6$, indicating that depending on σ and η the presence of the bulk polymers might cap the growth of the surface-bound layer. This observation is consistent with many experimental studies, in which the thickness of the polymer layer reaches a plateau value at long polymerization times.²⁶ The presence of this plateau has typically been attributed to excessive terminations during the polymerization, thus decreasing the density of the propagating radicals on the surface. This explanation alone, however, cannot hold true in our simulations due to the lack of termination reactions. We thus suggest that in addition to termination (and possible chain transfer) the plateau in $\langle N \rangle_S$ can be associated (at least in part) with (1) the competition for free monomers between the bulk- and surface-initiated macroinitiators (i.e., growing chains) and (2) the slower polymerization rate from the surface-initiated sites that, in turn, depends on the degree of confinement of the surface-grown macromolecule. Comparing $\langle N \rangle_B$ and $\langle N \rangle_S$ reveals the principal finding of this study, namely, that at a particular monomer conversion $\langle N \rangle_B - \langle N \rangle_S = \delta > 0$. The magnitude of δ depends on the combination of σ and η . Generally, δ decreases with decreasing σ and increasing η . These observations, on which we will elaborate more in the following sections, suggest that the common practice of associating the properties of surface-grown polymers with those polymerized in the bulk is of limited validity.

To understand the growth rate of both sets of polymers, we plot $\langle N \rangle_B$ ($\eta = 0\%$, left column) and $\langle N \rangle_S$ ($\eta = 100\%$, right column) as a function of MC step per bead (cf. Figure 2). The top row shows the raw data. As expected, increases in M_0 lead to higher rates of polymerization (initial slopes of the plots) and polymer molecular weights. The rate of polymerization of surface-grown polymers also depends on σ ; it decreases with increasing σ . Furthermore, the rate of polymerization for surface-initiated polymers at low σ is similar to that of the bulk-initiated chains. This reinforces the claim that at low σ and X_m low chain crowding on the surfaces results in similar growth for bulk- and surface-initiated polymers. Classical polymerization kinetics suggests that the rate of polymerization is proportional

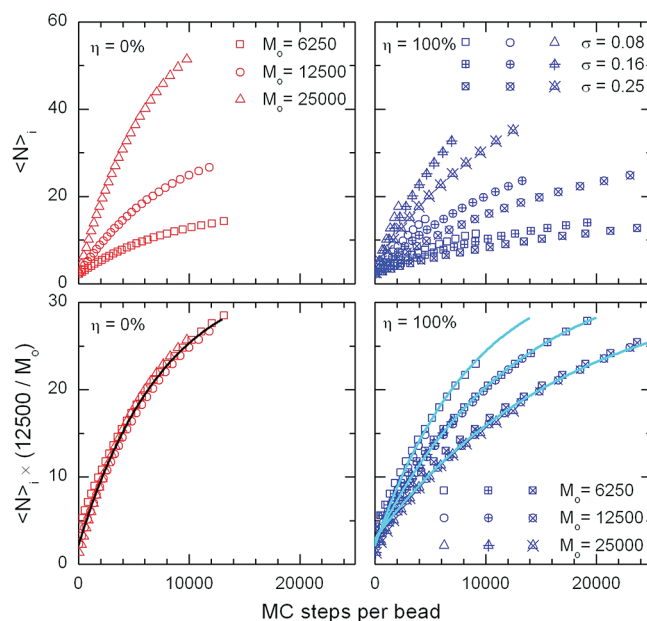


Figure 2. Number-average molecular weight (top row) and the same quantity scaled (bottom row) for bulk (left column, red, $\eta = 0\%$) and surface (right column, blue, $\eta = 100\%$) polymers as a function of Monte Carlo steps per bead for initial number of monomers (M_0): 6250 (squares), 12 500 (circles), and 25 000 (triangles); grafting density of initiators (σ): 0.08 (hollow), 0.16 (cross), and 0.25 (ex). The black and cyan lines are guides to the eye for the bulk- and surface-initiated data, respectively.

to the concentration of free monomers. To verify this, we use the $M_0 = 12\,500$ case as a benchmark and scale the data by multiplying by $12\,500/M_0$ (bottom row in Figure 2). All bulk data and surface data for a given value of σ overlap visually, confirming the rate dependence on M_0 and validate the choices of P_r and LT discussed earlier. Figure 3 shows the scaled data for various combinations of η , σ , and M_0 . A few trends can be identified by exploring the data in Figure 3. First, at $\sigma = 0.08$, the $\eta = 0\%$ (i.e., only bulk-initiated polymerization, black line) and $\eta = 100\%$ (i.e., only surface-initiated polymerization, cyan line) cases exhibit essentially the same growth rates. As σ increases and the surface chains start to crowd, we observe differences between the $\eta = 0\%$ and $\eta = 100\%$ cases; the surface growth rate slows down while the bulk growth rate remains fairly constant. Second, at low values of η , $\langle N \rangle_B$ traces perfectly the $\eta = 0\%$ line while $\langle N \rangle_S$ lies below the $\eta = 100\%$ line. At large values of η the opposite trend occurs; namely, $\langle N \rangle_S$ traces the $\eta = 100\%$ line closely (except at large monomer conversions) while $\langle N \rangle_B$ lies above the $\eta = 0\%$ line. The initial polymerization rates obtained by fitting a first-order exponential to the data ($X_m < 0.2$) and evaluating the derivative at $X_m = 0$ are plotted in Figure 4. We observe a dependence of the initial rate of polymerization on M_0 , indicating that not all of the rate variation is accounted for by scaling the data by M_0 . Two additional and somewhat related factors that may affect the rate of polymerization include (1) monomer diffusion limitation and (2) the percentage of accepted attempted moves. Diffusion limitation can arise if the monomer concentration decreases close to the surface or in proximity to the polymer chain ends. This effect results in lower polymerization rates as M_0 decreases. The move acceptance rate may affect the initial polymerization rates by perturbing the time unit in the simulation. Increasing M_0 , for example, results in an increase

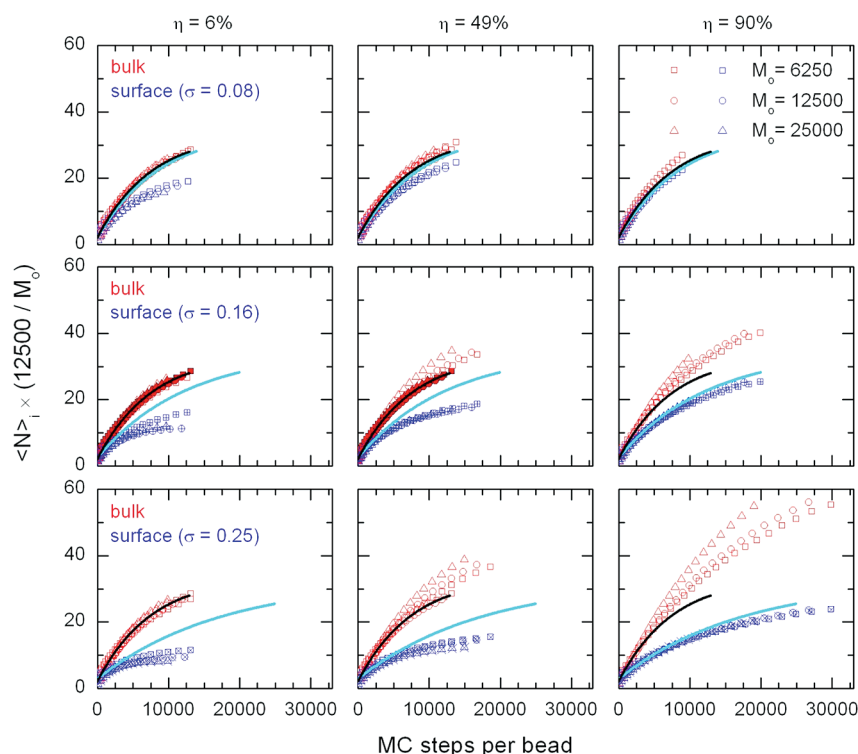


Figure 3. Scaled number-average molecular weight as a function of Monte Carlo step per bead for bulk (red) and surface (blue) polymers with fraction of surface polymers (η , left to right columns): 6%, 49%, and 90%; initiator grafting densities (σ , top to bottom rows): 0.08, 0.16, and 0.25; initial number of monomers (M_0): 6250 (squares), 12 500 (circles), and 25 000 (triangles). The solid lines correspond to $\eta = 0\%$ (black) and $\eta = 100\%$ (cyan).

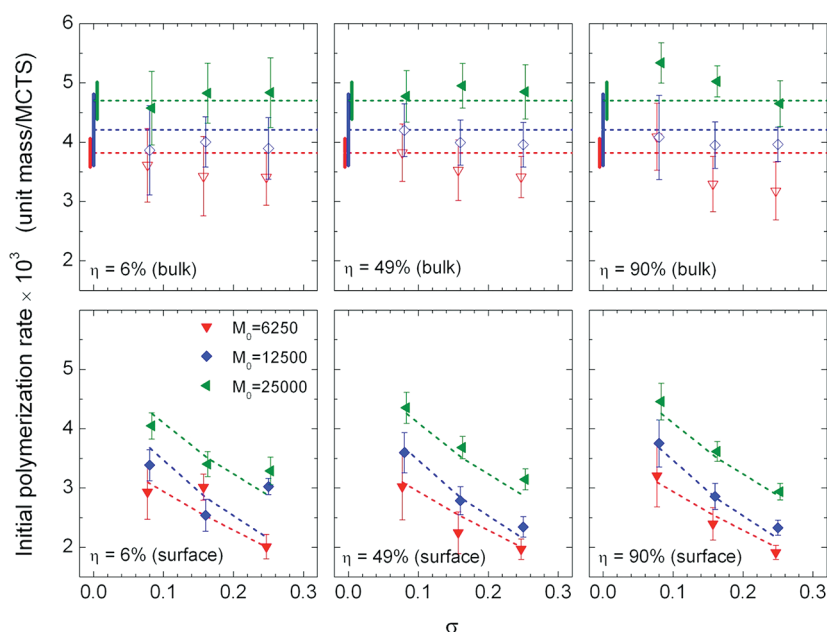


Figure 4. Initial polymerization rate as a function of σ for bulk (open symbols, top row) and surface (close symbols, bottom row) for η equal to 6% (left column), 49% (middle column), and 90% (right column) and M_0 equal to 6250 (red down triangle), 12 500 (blue diamond), and 25 000 (green left triangle). For clarity, the data for $M_0 = 6250$ and $M_0 = 25 000$ have been shifted horizontally by a small arbitrary increment to the left and right, respectively. The dotted lines in the top and bottom rows represent $\eta = 0\%$ (bulk-only polymerization) and 100% (surface-only polymerization), respectively. The solid vertical lines in the top row at $\sigma = 0$ denote the range of the $\eta = 0\%$ data.

of the lattice occupancy and therefore the probability of an attempted move to an already occupied lattice site. This would lead to a higher fraction of attempted moves being rejected resulting in slower motion. This effect would result in slower

polymerization rates for $M_0 = 25 000$ than for the systems with lower M_0 . Barring other factors, it appears that diffusion limitation may play a role in our simulations, although its effect on the rate of polymerization is small compared to that of the

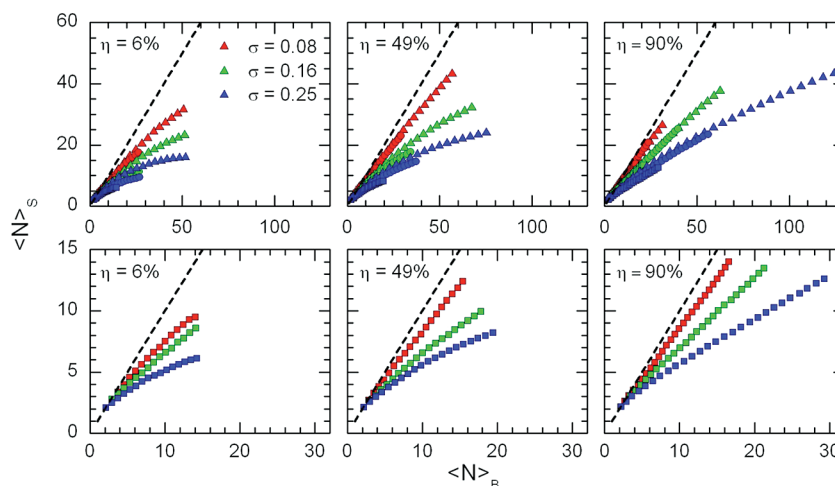


Figure 5. Number-average molecular weight of surface polymers as a function of number-average molecular weight of bulk polymers for the three values of M_0 (top row) and for $M_0 = 6250$ (bottom row). Percentage of surface polymers (η): 6% (left column), 49% (middle column), and 90% (right column); initial number of free monomers (M_0): 6250 (squares), 12 500 (circles), and 25 000 (triangles); grafting density of initiators (σ): 0.08 (red), 0.16 (green), and 0.25 (blue). The black dashed line represents $\langle N \rangle_s = \langle N \rangle_B$.

monomer concentration, M_0 . Figure 4 also depicts the dependence of the initial polymerization rate on σ for bulk- and surface-grown polymers. In most cases the rate of bulk polymerization is independent of σ (the sole exception being the $\eta = 90\%$ and $M_0 = 25\,000$ case). The bulk polymers, at least at the beginning of the reaction, are unaffected by the presence of the surface-growing polymers or by their grafting density. The surface-initiated polymers, however, do exhibit a polymerization rate dependence on σ as would be expected from the findings reported in our earlier publication.²² As σ increases, the rate of polymerization decreases consistently likely due to chain crowding at the surface.

To better discern the relation between the molecular weights of surface- and bulk-grown polymers at a particular instant of the polymerization reaction, in Figure 5 (top row) we plot the number-average molar weight of the surface grown polymers ($\langle N \rangle_s$) as a function of the number-average molar weight of the bulk polymers ($\langle N \rangle_B$). The black dashed lines correspond to $\langle N \rangle_B = \langle N \rangle_s$. For all combinations of σ , η , and M_0 , the data lie below the diagonals, indicating that $\langle N \rangle_s < \langle N \rangle_B$ at all conversions. An important characteristic of these systems is the competition for free monomers between the bulk- and surface-grown polymers and the higher growth rate of the bulk polymers relative to the surface ones. This is a clear indication that confining the initiators on the flat impenetrable surface reduces the rate of polymerization. As the density and confinement of the initiators on the surface increases, the difference between the growth rates of the surface and bulk polymers widens yielding shorter surface-bound macromolecules relative to free chains initiated in bulk. The data in Figure 5 suggest that in the limit of low σ and high η the $\langle N \rangle_B = \langle N \rangle_s$ assumption is valid. Unfortunately, most experiments employing simultaneous bulk and surface initiators operate at low values of η instead.

By inspecting the top row of Figure 5, we observe that the data lie closer to the diagonal on going from $\eta = 6\%$ to $\eta = 90\%$ (from left to right). This observation is counterintuitive since we invoke confinement and crowding as the reasons for the difference between $\langle N \rangle_B$ and $\langle N \rangle_s$. As explained before, the confinement on the surface for all values of η is identical as long as σ remains constant. One would expect that an increase in η

would have no effect in the deviation of the data from the diagonal. We explain this behavior by the presence (or lack thereof) of the fast growing polymers in the bulk. At $\eta = 6\%$ most of the polymers in the simulation are fast-growing bulk polymers. Increasing the amount of these fast growing polymers, relative to the polymers attached to the surface, results in larger differences between $\langle N \rangle_B$ and $\langle N \rangle_s$. At high η , the slow-growing surface polymers outnumber the bulk polymers. Although the bulk polymers possess a faster growing rate per chain, as a group they add fewer monomers than the surface-based chains. This then results in the observed shift of the trends toward the diagonal and the better match between $\langle N \rangle_B$ and $\langle N \rangle_s$ at large values of η .

An interesting trend to note from Figure 5 is the behavior of the final values of $\langle N \rangle_B$ and $\langle N \rangle_s$ at $X_m = 0.80$ as a function of σ and η for the $M_0 = 6250$ case (bottom row). At $\eta = 6\%$, $\langle N \rangle_B$ ($X_m = 0.80$) remains nearly constant at a value of ≈ 12 with increasing σ . However, as σ increases, $\langle N \rangle_s$ decreases from ≈ 10 to ≈ 7 . At $\eta = 90\%$ $\langle N \rangle_B$ is more sensitive to increasing σ than $\langle N \rangle_s$; $\langle N \rangle_s$ decreases from ≈ 14 to ≈ 13 , and $\langle N \rangle_B$ increases from ≈ 17 to ≈ 30 . The latter observation is intriguing because one would not expect σ , which is a property of the surface, to have such a large effect on $\langle N \rangle_B$ ($X_m = 0.80$). To explain this behavior, we have to take into consideration three factors: (1) the effect of crowding/confinement on the rate of surface polymerization, (2) the relative rates of surface and bulk growth, and (3) the ratio of bulk polymers to free monomers. The slight variation in $\langle N \rangle_B$ with σ at $\eta = 6\%$ is explained by noting that the surface in this system constitutes a small perturbation and therefore cannot inflict a large effect on the bulk-based polymers. The differences in $\langle N \rangle_s$ are due to the crowding and slowing down of the surface-initiated reaction at higher σ .²² For $\eta = 90\%$, the decrease in $\langle N \rangle_s$ is still explained by the effects of surface confinement. The large increase in $\langle N \rangle_B$, however, is interesting and more complex to explain. In this system, the surface plays a very significant role because this is where most of the polymers are located. As σ increases, the rate of polymerization of the surface-initiated polymers slows down and because surface-initiated polymers represent the majority component; the overall rate of polymerization decreases as well. In contrast to $\eta = 6\%$, at $\eta = 90\%$ the bulk

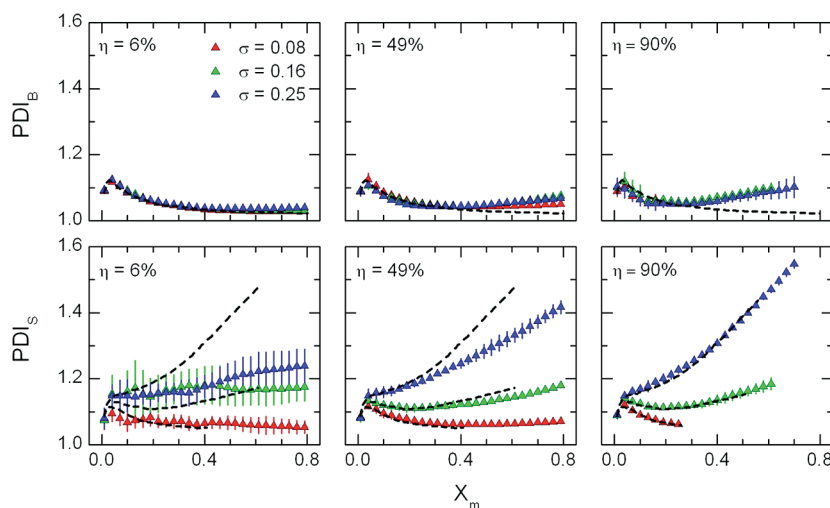


Figure 6. Polydispersity index for bulk (top row) and surface (bottom row) polymers as a function of monomer conversion with initial number of monomers (M_0) of 25 000; percentages of surface polymers (η): 6% (left column), 49% (middle column), and 90% (right column); grafting densities of initiators (σ): 0.08 (red), 0.16 (green), and 0.25 (blue). The black dashed lines represent the $\eta = 0\%$ (top row) and $\eta = 100\%$ (bottom row), $M_0 = 25\,000$ and $\sigma = 0.08$, 0.16, and 0.25 conditions.

polymers only compete with the slow-growing surface-based polymers. The same trends are expected for higher values of M_0 although they cannot be observed here due to the aforementioned truncation of the data sets at $\eta = 90\%$ (cf. Table SI).

As mentioned above, our aim is to explore the consequences of these findings on the common experimental practice that assumes similar properties between polymers grown simultaneously in bulk and on the surface and using the molecular weight of the bulk-based macromolecules to estimate σ . The typical approach involves measuring the dry thickness of the polymer layer by means of optical ellipsometry or neutron/X-ray reflectivity and employing eq 1, in which $M_{n,S}$ ($= \langle N \rangle_S$) is determined by SEC. As can be seen in Figure 5, the only situation in which this assumption is approximately valid is for small values of σ on flat substrates and for small fraction of bulk-initiated polymers. At high σ , the differences between $\langle N \rangle_B$ and $\langle N \rangle_S$ are likely to be larger than the error of the SEC measurement, resulting in inaccurate estimates of σ . These results highlight the need for continued development of direct measurement experimental techniques of either $\langle N \rangle_S$ or σ .

Simultaneous polymerization of bulk-based and surface-anchored initiators also influences the broadness of the molecular weight distributions of both populations of polymers. In Figure 6 we plot the PDI of bulk (PDI_B , top) and surface (PDI_S , bottom) polymers as a function of X_m , η , and σ for $M_0 = 25\,000$. At low η , the PDI_B resembles very closely the situation corresponding to the $\eta = 0\%$ case for all values of σ . As η increases, the PDI deviates above the $\eta = 0\%$ line at approximately $X_m = 0.3$. This provides an additional indication that when the surface polymers constitute the majority component in the simulation they can affect the properties of the bulk-initiated polymers. The surface polymers exhibit the opposite trend; namely, that at $\eta = 90\%$, their PDI values are nearly identical to those corresponding to the polymerization at $\eta = 100\%$, and as η decreases, the PDI_S values for σ equal to 0.16 and 0.25 decrease below the $\eta = 100\%$ line. This is difficult to see in the $\eta = 6\%$ case because the error in the PDI of a small number of polymers is significant. At a particular conversion and for $\eta = 6\%$ and 49%, the presence of bulk polymers imparts

a lower PDI to the surface-grown polymers. Although this observation is intriguing, it is misleading, as we will explain below (Figure 8).

The data in Figure 7 show the evolution of the PDI of the bulk and surface polymers as a function of monomer

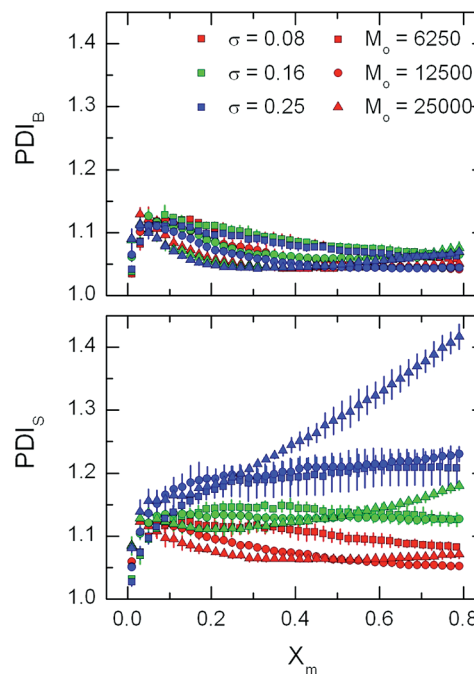


Figure 7. PDIs of bulk (top) and surface (bottom) polymers as a function of the monomer conversion for $\eta = 49\%$. Initiator grafting densities (σ): 0.08 (red), 0.16 (green), and 0.25 (blue); initial number of free monomers (M_0): 6250 (squares), 12 500 (circles), and 25 000 (triangles).

conversion for $\eta = 49\%$ and M_0 equal to 6250, 12 500, and 25 000. When plotted against X_m , one can see how the results of a hypothetical SEC experiment would depict the broadness of the distributions at any time during the polymerization reaction. At $\sigma = 0.08$, the assumption that the PDI obtained for

the bulk polymers is similar to that of polymers initiated from the surface is reasonable. However, as σ increases to 0.25, this assumption ceases to be valid and PDI_s becomes much larger than PDI_b for all values of M_0 . At $X_m = 0.8$ and $M_0 = 25\,000$ the difference in the PDI of the surfaces from that of the bulk is ~ 0.3 . A change of this magnitude in the PDI will most certainly alter the properties of the surface-grown polymer layers²⁷ (thickness, density, etc.) and therefore their performance in practical applications that rely on monodisperse polymer chains²⁸ (i.e., antifouling coatings). These observations suggest that in order to assume that the simultaneously grown bulk and surface polymers possess similar properties it is necessary to know the value of σ precisely. As described above, estimation of σ requires that the properties between bulk and surface polymers be similar, resulting in a circular problem. The differences between the molecular weight distributions are evident when plotted as PDI_s vs PDI_b (cf. Figure S2 in Supporting Information).

One motivation to explore polymerizations with different values of M_0 is the possibility that $\langle N \rangle_s$ has an effect on the growth rate and PDI of polymers grown from flat surfaces. For instance, at the beginning of the polymerization process when $\langle N \rangle_s$ is low, the surface-based polymers grow with little or no crowding. With increasing polymerization time, the molecular weight of the macromolecular grafts increases and neighboring chains approach one another. At some point, excluded volume interactions will cause chain stretching away from the surface. In addition, chain crowding among neighbors may hinder the delivery of monomers to the chains with conformations in which the chain ends reside inside the polymer layer. Whereas plotting the PDIs as a function of X_m elucidates the differences between bulk and surface polymers at a particular instant during the polymerization, this plot masks the dependence that the PDI may have on the average molecular weights. A plot of the PDI as a function of the average molecular weight of the polymers can document this type of dependency effectively (cf. Figure 8). When plotted against $\langle N \rangle_b$ and $\langle N \rangle_s$, the PDI_b and PDI_s are independent of M_0 because for a given value of $\langle N \rangle_b$ or $\langle N \rangle_s$ we consider the same number of beads in the bulk- or surface-based polymer, respectively, regardless of the solution conditions. The bulk polymers also prove to be insensitive to σ , indicating that no matter what the characteristic of the surface are, the bulk polymers that grow to a particular molecular weight possess similar PDIs. The surface-grown polymers, however, do exhibit a dependence on σ as should be expected from our earlier study.²² As σ increases, the PDI_s increases due to chain crowding resulting in the uneven delivery of monomers to the short and long chains. This insensitivity of the PDI to the value of M_0 can explain the observed decrease in PDI_s when most of the growing polymers are in the bulk ($\eta = 6$ and 49%, Figure 6) relative to the case rich in surface polymers. This is in fact due to the fast growing polymers leading to lower $\langle N \rangle_s$ at a particular conversion and therefore a lower level of confinement and observed PDI_s .

In this work, we have established that η and σ have a strong effect on the MWDs of bulk- and surface-grown polymers and that knowing these parameters is essential for the validation of the $\langle N \rangle_b \approx \langle N \rangle_s$ assumption. We now draw parallels between the range of σ and η studied here and those found in the experimental literature. Experiments where the initiation of surface polymerization occurs from a planar substrate operate often at very low values of η (or $\eta = 0\%$, i.e., no sacrificial initiator) due primarily to the low surface area of the planar

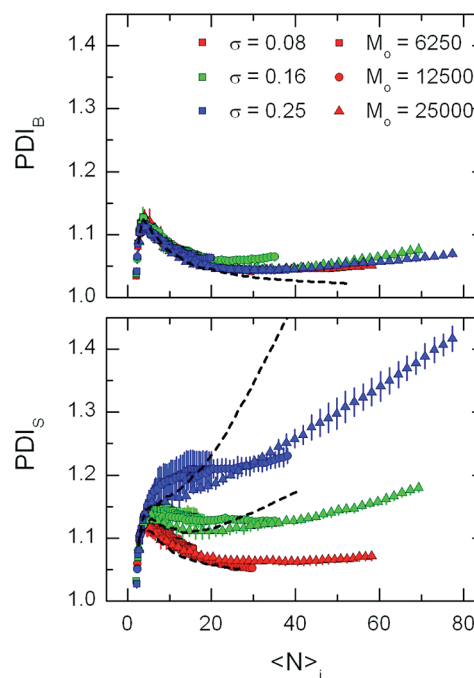


Figure 8. PDIs of bulk (top) and surface (bottom) polymers as a function of the average molar mass of bulk and surface polymers, respectively, for $\eta = 49\%$. Initiator grafting densities (σ): 0.08 (red), 0.16 (green), and 0.25 (blue); initial number of free monomers (M_0): 6250 (squares), 12 500 (circles), and 25 000 (triangles). The black dashed lines represent the $\eta = 0\%$ (top) and $\eta = 100\%$ (bottom), $M_0 = 25\,000$ and $\sigma = 0.08, 0.16$, and 0.25 conditions.

sample. Thus, the determination of σ encounters problems outlined in this paper. For example, Husseman et al.¹⁸ and Koylu and Carter²⁹ performed their experiments at $\eta \ll 0.0001\%$ and 0.01% , respectively. The values of σ calculated by the authors in these studies ranged from 0.5 to 1.4 chains/nm². Koylu and Carter concluded that the assumption of equal bulk and surface average molecular weights is not universally valid based on their SEC measurements of the grafted and solution chains. Specifically, Koylu and Carter reported a lower molecular weight of polymers grown in solution relative to those polymerized from the substrate, which is opposite to the trend described here. Based on their computed values of σ (≈ 1.0 chain/nm²), the estimated value of η cited above, and the data in Figure 3, one would expect the average molecular weight on the surface to be substantially smaller than that in the bulk. The discrepancy may lie in the nature of the substrate in the work of Koylu and Carter. Instead of an impenetrable surface confining the initiators to a two-dimensional plane, the initiators were bound to a three-dimensional photopolymer film. Husseman and co-workers did not measure the molecular weight of polymer brushes grown from planar substrates. Instead, their results showed similar molecular weights and PDIs between polymer cleaved from silica gel particles and those free in solution. The positive convex curvature of the substrate may have contributed to a relatively low PDI of the surface-initiated polymers due to lower chain crowding relative to that seen in flat substrate geometries. A comparison to polymers grown from the substrate is thus not appropriate unless one works with very low values of σ or very small curvatures. Jeyaprakash et al. compared ATRP polymerizations with added deactivators ($\eta = 100\%$) and with sacrificial initiators (η unknown) and showed that polymerizations in the

presence of deactivators produce thicker grafted layers than those carried out in the presence of free initiators.²⁶ The explanation Jeyaprakash and co-workers put forth is consistent with our observations; i.e., η affects the rate of polymerization of the surface-initiated polymers and can therefore lead to polymers with $\langle N \rangle_S \neq \langle N \rangle_B$.

Silica-based mesoporous materials can also serve as supports for surface initiated CRP studies. In this case, it is possible to cleave sufficient amount of polymeric material from the substrate for subsequent SEC analysis. However, the negative curvature of the initiator-covered surfaces and the diffusion of monomer to the pores may accentuate the effects observed in this study. Kruk et al.³⁰ performed such polymerizations at $\eta = 0\%$ and noted that the polymerization was controlled and the PDI remained as small as in solution based ATRP (<1.1). Pasetto³¹ and co-workers, however, carried out polymerizations from similar mesoporous materials over a whole range of η and noted higher PDIs and lower molecular weights for the surface-bound polymers. Similar conclusions have been reached in the study of Gorman and co-workers although simultaneous bulk polymerizations were not carried out.³² This inconsistency of observations for both planar substrates and mesoporous materials highlights the need for continued research in the area and for a systematic investigation of the effects of η and σ in the controlled growth of polymer chains. The simulations performed here can serve as a guide to the proper design of such investigation.

CONCLUSIONS

The computer simulations implemented herein provide insight into the competitive growth of macromolecules initiated simultaneously in the bulk and on flat surfaces. We observe that the common assumption invoked in the literature of equality between the molecular weights of the bulk ($\langle N \rangle_B$)- and surface ($\langle N \rangle_S$)-based polymers is generally invalid. We find that in most instances $\langle N \rangle_B > \langle N \rangle_S$. Furthermore, the broadness of the molecular weight distribution of surface-grown polymers is highly dependent on their grafting density (σ), suggesting that claims, often found in the literature, of narrowly distributed surface-grown polymers polymerized by means of living polymerization are not generally valid.

We confirm that σ has an important effect on the growth rate and polydispersity of surface-grown polymers. Depending on the percentage of polymers on the surface (η), the properties of the bulk polymers are also affected by σ , which is a surface property. When η is large, the surface represents a strong perturbation to the growth of bulk polymers; as a consequence, the molecular weights of the bulk polymers at a monomer conversion of 0.8 increase with increasing σ . This behavior is attributed to the fact that at low η the bulk polymers compete with each other (they are the majority component) while at high η they compete primarily with the slow-growing surface-initiated polymers. By performing simulations at various initial numbers of free monomers (M_0), we confirm that the initial rate of polymerization is proportional to M_0 . However, diffusion limitation likely affects the polymerization; this effect becomes less important with increasing M_0 . The initial rates of polymerization also depend on σ . Increasing σ results in decreases in the rate of polymerization, confirming the results presented earlier.¹⁶

In the present work we utilized the canonical (NVT) ensemble. A more realistic model would require implementing the grand canonical ensemble that would describe a situation

involving a constant chemical potential of the free monomers in solution. The latter is encountered in a typical experimental setup. We note, however, that the general conclusions reached here should still be valid even in the grand canonical ensemble. Namely, the molecular weight of bulk-initiated polymers should be higher than that of polymer brushes grown from surfaces. In fact, given the constant large excess of monomers in the reservoir, the differences between $\langle N \rangle_S$ and $\langle N \rangle_B$ and the corresponding PDI of both families of polymers will likely be higher than those reported herein.

ASSOCIATED CONTENT

Supporting Information

Description of the lattice employed in MC BFM simulations for various values of σ and η , plots of PDI_S vs PDI_B , and details of the data truncation. This material is available free of charge via the Internet at <http://pubs.acs.org>.

AUTHOR INFORMATION

Corresponding Author

*E-mail Jan_Genzer@ncsu.edu, Tel +1-919-515-2069.

Present Address

[†]School of Chemical & Biomolecular Engineering, Cornell University, Ithaca, NY 14853-5201.

Notes

The authors declare no competing financial interest.

ACKNOWLEDGMENTS

We thank the National Science Foundation for supporting this work through Grant DMR-0906572.

REFERENCES

- (1) Barbey, R.; Lavanant, L.; Paripovic, D.; Schüwer, N.; Sugnaux, C.; Tugulu, S.; Klok, H.-A. *Chem. Rev.* **2009**, *109*, 5437–527.
- (2) Jones, D. M.; Smith, J. R.; Huck, W. T. S. *Adv. Mater.* **2002**, *13*, 1130–1134.
- (3) Jones, D. M.; Huck, W. T. S. *Adv. Mater.* **2001**, *13*, 1256.
- (4) Matyjaszewski, K.; Dong, H.; Jakubowski, W.; Pietrasik, J.; Kusumo, A. *Langmuir* **2007**, *23*, 4528–4531.
- (5) Gautrot, J. E.; Trappmann, B.; Ocegüera-Yanez, F.; Connelly, J.; He, X.; Watt, F. M.; Huck, W. T. S. *Biomaterials* **2010**, *31*, 5030–41.
- (6) Moglianetti, M.; Webster, J. R. P.; Edmondson, S.; Armes, S. P.; Titmuss, S. *Langmuir* **2010**, *26*, 12684–9.
- (7) Takahashi, H.; Nakayama, M.; Yamato, M.; Okano, T. *Biomacromolecules* **2010**, *11*, 1991–9.
- (8) Advincula, R. C. In *Polymer Brushes*; Advincula, R. C., Brittain, W. J., Caster, K. C., Rühle, J., Eds.; Wiley-VCH Verlag GmbH & Co. KGaA: Weinheim, 2004; p 501.
- (9) Zhao, B.; Brittain, W. J. *Prog. Polym. Sci.* **2000**, *25*, 677–710.
- (10) Brittain, W. J.; Minko, S. J. *Polym. Sci., Part A: Polym. Chem.* **2007**, *45*, 3505–3512.
- (11) Jones, D. M.; Brown, A.; Huck, W. *Langmuir* **2002**, *18*, 1265–1269.
- (12) Baum, M.; Brittain, W. J. *Macromolecules* **2002**, *35*, 610–615.
- (13) Kim, J.-B.; Huang, W.; Bruening, M. L.; Baker, G. L. *Macromolecules* **2002**, *35*, 5410–5416.
- (14) Brinks, M. K.; Studer, A. *Macromol. Rapid Commun.* **2009**, *30*, 1043–1057.
- (15) Ye, Q.; Wang, X.; Li, S.; Zhou, F. *Macromolecules* **2010**, *43*, 5554–5560.
- (16) Matyjaszewski, K.; Xia, J. *Chem. Rev.* **2001**, *101*, 2921–2990.
- (17) Pyun, J.; Kowalewski, T.; Matyjaszewski, K. *Macromol. Rapid Commun.* **2003**, *24*, 1043–1059.

- (18) Husseman, M.; Malmström, E. E.; McNamara, M.; Mate, M.; Mecerreyes, D.; Benoit, D. G.; Hedrick, J. L.; Mansky, P.; Huang, E.; Russell, T. P.; Hawker, C. J. *Macromolecules* **1999**, *32*, 1424–1431.
- (19) Tomlinson, M. R.; Efimenko, K.; Genzer, J. *Macromolecules* **2006**, *39*, 9049–9056.
- (20) Turgman-Cohen, S.; Genzer, J. *J. Am. Chem. Soc.* **2011**, *133*, 17567–17569.
- (21) Genzer, J. *Macromolecules* **2006**, *39*, 7157–7169.
- (22) Turgman-Cohen, S.; Genzer, J. *Macromolecules* **2010**, 101022125807042.
- (23) Carmesin, I.; Kremer, K. *Macromolecules* **1988**, *21*, 2819–2823.
- (24) Deutsch, H.; Binder, K. *J. Chem. Phys.* **1991**, *94*, 2294–2304.
- (25) Goto, A.; Fukuda, T. *Prog. Polym. Sci.* **2004**, *29*, 329–385.
- (26) Jeyapragash, J. D.; Samuel, S.; Dhamodharan, R.; Riihe, J. *Macromol. Rapid Commun.* **2002**, *23*, 277–281.
- (27) de Vos, W. M.; Leermakers, F. A. M. *Polymer* **2009**, *50*, 305–316.
- (28) de Vos, W. M.; Leermakers, F. A. M.; de Keizer, A.; Kleijn, J. M.; Cohen Stuart, M. A. *Macromolecules* **2009**, *42*, 5881–5891.
- (29) Koylu, D.; Carter, K. R. *Macromolecules* **2009**, *42*, 8655–8660.
- (30) Kruk, M.; Dufour, B.; Celer, E. B.; Kowalewski, T.; Jaroniec, M.; Matyjaszewski, K. *Macromolecules* **2008**, *41*, 8584–8591.
- (31) Pasetto, P.; Blas, H.; Audouin, F.; Boissière, C.; Sanchez, C.; Save, M.; Charleux, B. *Macromolecules* **2009**, *42*, 5983–5995.
- (32) Gorman, C. B.; Petrie, R. J.; Genzer, J. *Macromolecules* **2008**, *41*, 4856–4865.